

Differences in Functional Clustering of Endogenous and Exogenous Substrates Between Members of the CYP1A Subfamily

Supplementary Material

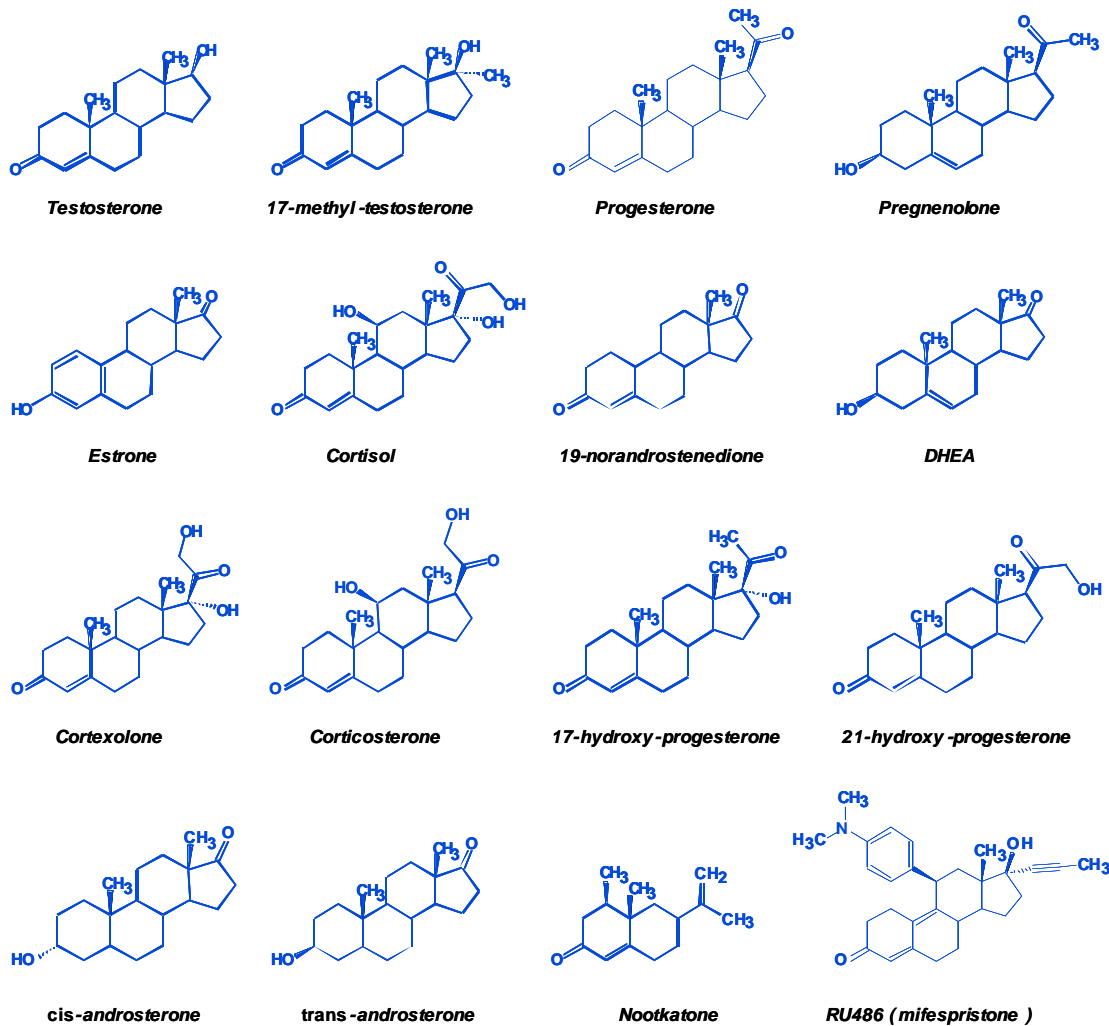


Fig. (S1). Structure of the steroid substrates used in this work.

Table S1. Observed rates of metabolite formation measured at a saturating concentration of steroid substrates. Metabolites were quantified by mass spectrometry after HPLC separation. Activities (units are $\mu\text{V}\cdot\text{s}/\text{min}/\text{mg}$ of microsomal protein) were calculated from initial velocities determined from metabolite concentration observed at different incubation times. The mammalian CYP1A enzymes were assayed in duplicate. An artificial mouse CYP1A1 - rabbit CYP1A2 chimera, the chimera 1ACh4, was also included. Enzymes were produced in yeast and incubations were performed with yeast microsomal fractions. This table is a non-processed data set

Testosterone			RU486				17-methyl-testosterone				Cortexolone				
T1	T2	T3	RU1	RU2	RU3	RU4	RU5	MT1	MT2	MT3	MT4	CTX1	CTX2		
Hum 1A1-1	15986.6	142577.1	1693.1	207786.2	4229.5	74994	2682.8	5838.6	9044.8	113258.7	9658.6	8013.3	13116.4	50786.9	
Hum 1A1-2	13320.3	118495.8	1407.1	336744.8	8750.9	54332	5061.3	10314.0	15129.7	118540.1	5619.6	12766.3	14679.8	68563.3	
Hum 1A2-1	8.9	2028.5	8.9	11259.9	5.7	5.7	5.7	5.7	8.2	8.2	8.2	11.6	11895.9		
Hum 1A2-2	8.9	3658.9	8.9	19089.3	5.7	5.7	5.7	5.7	8.2	8.2	8.2	8.2	11.6	9115.4	
Mou 1A1-1	1588.8	67225.1	8.9	359506.6	5.7	5.7	5.7	5.7	1422.3	8.2	81412.3	8564.7	2429.0	28459.8	46343.1
Mou 1A1-2	980.2	45669.4	8.9	173040.0	5.7	5.7	5.7	5.7	967.0	8.2	53643.5	5378.3	4163.0	14154.4	14347.3
Rab 1A2-1	3596.5	82741.9	2103.9	1447504.5	5.7	5.7	5.7	5.7	8.2	8.2	63275.1	6716.7	1418.8	23720.8	61822.6
Rab 1A2-2	897.3	27970.9	23695	363536.2	5.7	5.7	5.7	5.7	8.2	8.2	36413.1	5792.7	1771.7	7307.9	19680.3
1ACh4	8.9	67955.8	4901.1	262670.3	5.7	5.7	5.7	5.7	665.5	8.2	79862.1	8382.6	5004.9	11.6	37463.7
Progesterone			Corticosterone				Pregnenolone				17-hydroxy-progesterone		DHEA		
PROG1	PROG2	PROG3	PROG4	PROG5	CTC1	CTC2	PREG1	PREG2	PREG3	PREG4	17HP1	17HP2	DH1		
Hum 1A1-1	370480.7	281494.4	394305	221005	16171.6	20736.9	114565.3	259450.6	53248.9	58124.5	72860.5	35823.1	10599.6	17936.6	
Hum 1A1-2	285911.5	161149.2	22178.4	17003.9	13193.8	18948.7	71962.2	114860.5	22341.2	32804.7	88967.8	12512.7	11890.2	76904	
Hum 1A2-1	9.2	1315.8	2142.7	4292.6	19844.3	8.7	8.7	21.5	21.5	21.5	12.7	12.7	13.6		
Hum 1A2-2	9.2	1493.5	2431.1	2845.9	13156.3	8.7	8.7	21.5	21.5	21.5	12.7	12.7	13.6		
Mou 1A1-1	42550.1	158594.5	27784.1	12352.3	11663.8	17719.1	36029.6	16233.9	21.5	8397.0	21.5	11071.2	12.7	99728	
Mou 1A1-2	15884.1	84049.1	5565.1	11272	12436.6	8590.2	23908.0	14379.8	21.5	10115.9	21.5	14179.8	12.7	4011.2	
Rab 1A2-1	62340.4	226850.1	57741.0	49273.0	15679.9	24031.0	24289.1	9420.6	21.5	65718.9	17786.5	12.7	9394.7		
Rab 1A2-2	14950.1	105378.6	19904.8	18032.2	2000.7	4930.7	11366.5	8927.0	21.5	15982.8	1649.3	12.7	1550.6		
1ACh4	44029.9	171292.0	23072.1	5381.4	21657.4	36242.6	35247.7	27686.7	4594.4	21.5	16958.7	12.7	13335.1		
DHEA		21-hydroxy-progesterone				Estrone				Nootkatone					
DH2	DH3	21HP1	21HP2	21HP3	21HP4	EST1	EST2	NK1	NK2	NK3	NK4	NK5	NK6		
Hum 1A1-1	14918.4	10735.9	41593.3	7968.3	16717.7	6.8	925421.8	562	18217.7	73782	33690.7	61102	37762.6	225429.4	
Hum 1A1-2	14262.8	11507.1	16951.1	3140.8	168230.9	6.8	691001.1	562	19410.3	553213.3	21881.9	5247.4	33906.2	119705.2	
Hum 1A2-1	13.6	29732.0	6.8	6.8	6.8	6491.1	6.8	56.2	56.2	7.8	7.8	7.8	7.8		
Hum 1A2-2	13.6	8827.5	6.8	6.8	6.8	12780.8	6.8	56.2	56.2	7.8	7.8	7.8	7.8		
Mou 1A1-1	7770.7	13.6	24070.9	6.8	24463.5	3025.1	422958.4	56153.0	7001.7	7.8	9526.2	7.8	10223.3	133203.7	
Mou 1A1-2	3125.7	13.6	7816.6	6.8	16267.3	6413.6	202036.0	57058.5	4328.6	7.8	5890.0	7.8	10783.4	66713.9	
Rab 1A2-1	6137.1	23499.7	60198.0	6.8	49081.4	10265.4	34488.2	56.2	7.8	7.8	26930.9	7.8	73688.3		
Rab 1A2-2	1640.4	7808.8	26470.0	6.8	19427.8	1787.4	14083.2	56.2	7.8	7.8	8648.7	7.8	6309.3	23465.8	
1ACh4	12540.8	13.6	22622.3	6.8	24688.0	6.8	478144.0	7.8	7.8	7.8	7535.4	7.8	10630.2	122072.5	
Nootkatone		Cortisol				cis -Androsterone				Norandrostenedione				trans -Androsterone	
NK7	NK8	HCl	cAD1	cAD2	cAD3	cAD4	NAD1	NAD2	NAD3	NAD4	NAD5	IAD1	IAD2		
Hum 1A1-1	33744.4	22725.2	50649.0	11271.7	4723.5	86624.0	15.8	63350.3	64238.3	5.2	7661.0	6831.3	32122.7	31906.1	
Hum 1A1-2	15926.6	22725.2	34940.8	4627.2	8445.5	4510.3	15.8	38837.8	21644.7	5.2	4570.3	4075.4	113285	24377.3	
Hum 1A2-1	7.8	34303.7	13.2	15.8	14560.8	38146.9	15.8	9322.9	19108.4	27342.9	5.2	3925.5	18.1	20223.8	
Hum 1A2-2	7.8	7036.7	13.2	15.8	6587.7	6061.6	15.8	10944.7	22433.2	32100.7	5.2	4611.5	18.1	9882.7	
Mou 1A1-1	19040.8	9186.2	17901.5	8377.6	4998.4	39532.4	15.8	24894.1	14065.8	5.2	776.6	1449.0	2146.2	7065.0	
Mou 1A1-2	5044.3	2739.2	79094	3050.6	15.8	49447.1	15.8	13882.3	8942.9	5.2	1141.9	2130.8	3115.5	10386.3	
Rab 1A2-1	8950.5	56109.4	37051.1	14475.5	7181.7	87842.0	6748.8	64875.9	30281.6	5.2	9783.0	3243.1	6729.2	60889.9	
Rab 1A2-2	7.8	11541.2	7214.3	4970.0	1582.9	45154.8	3376.0	27400.2	14894.1	5.2	4629.2	2866.8	19025.3	32424.2	
1ACh4	17363.5	778.0	28039.8	8884.7	5128.0	76453.4	15.8	29745.5	59857.4	5.2	5.2	3794.2	12485.6		

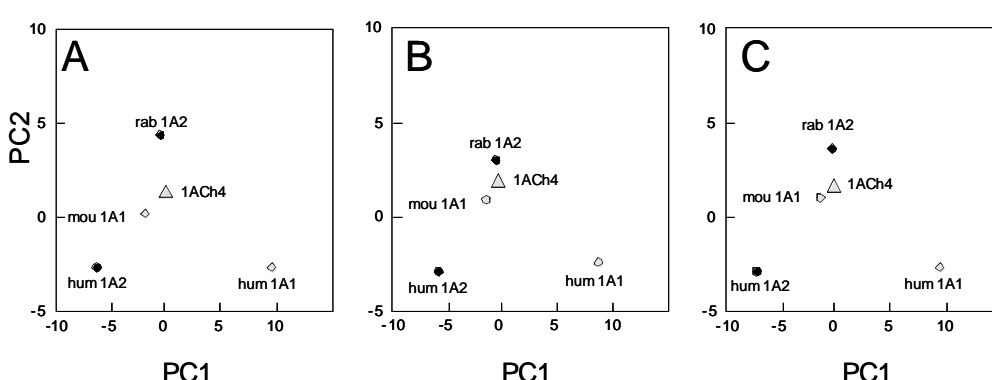


Fig. (S2). Comparison of the principal component analyses on steroid dataset obtained with three different normalization procedures. (A). No normalization. (B). Normalization by the variance. (C). Normalization by the average substrate peak area. The first principal component accounts for 53.5 % of the variance in the initial dataset for panel A and for 60.2 % for both panels B and C. Grey circles, 1A1s; solid circles, 1A2s; grey triangle, chimera 1ACh4 (mostly mouse 1A1).

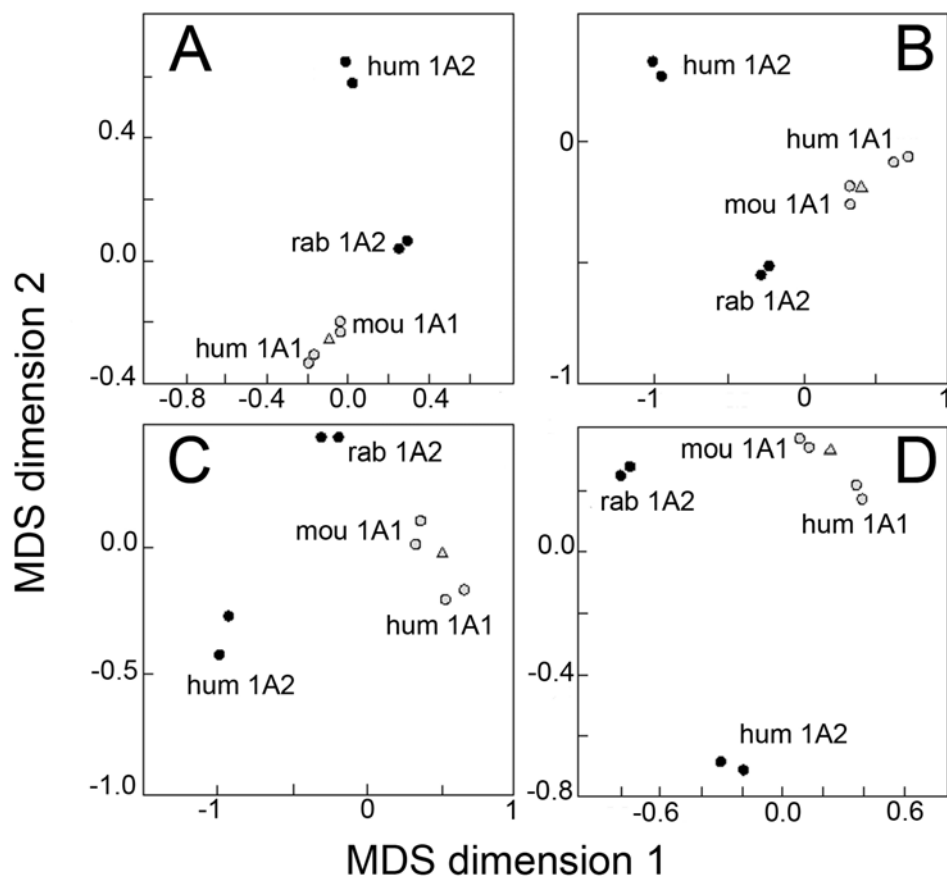


Fig. (S3). Comparison of MDS configuration plots obtained with four different models applied on steroid activity data. (A). Ratio MDS model, *stress* = 0.064. (B). Absolute MDS model, *stress* = 0.063. (C). Interval MDS model, *stress* = 0.064. (D). Polynomial MDS model, *stress* = 0.123. CYP1A1, grey; CYP1A2, black; chimera 1ACh4, triangle.

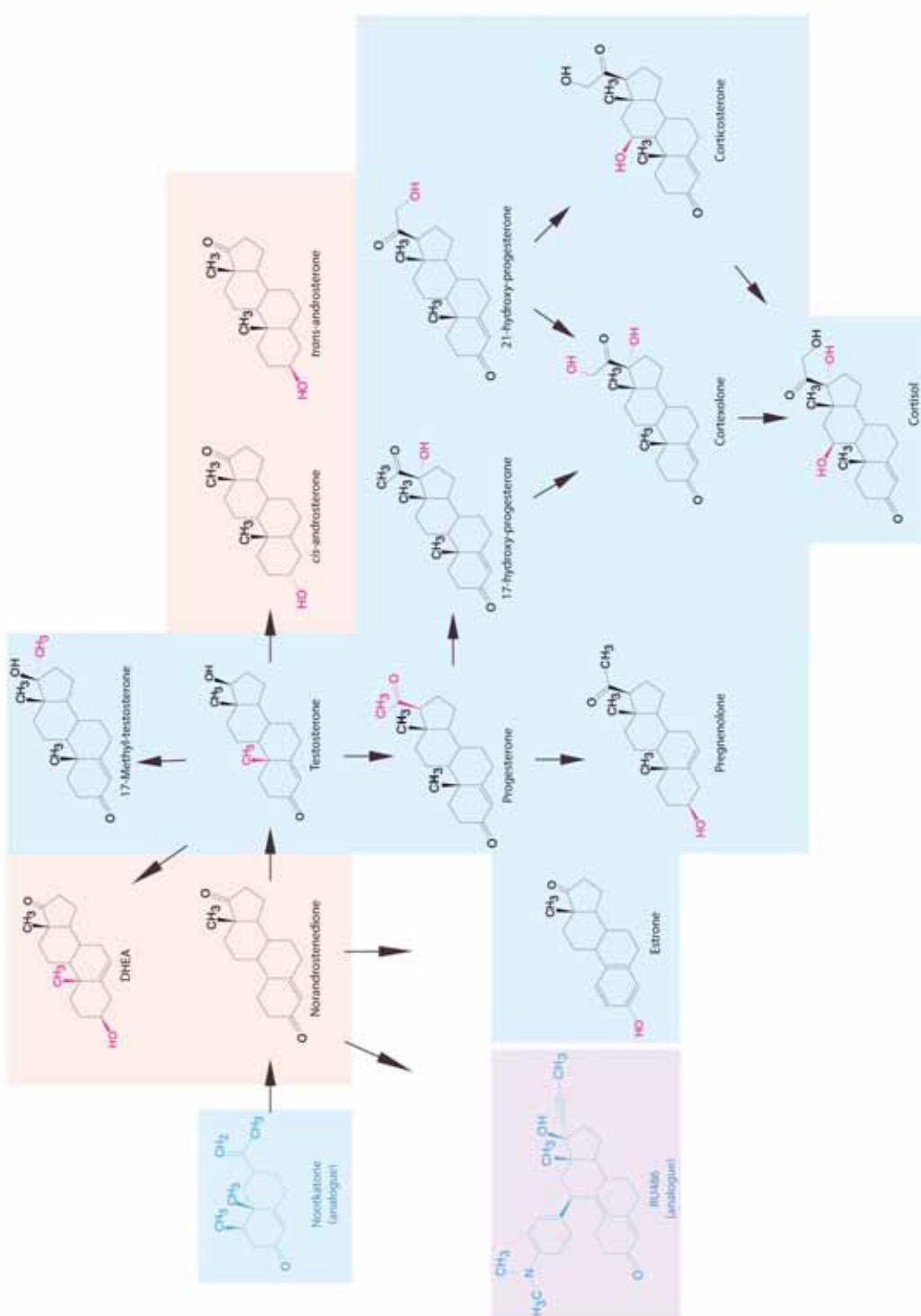


Fig. (S4). Step by step comparison of steroid and analogues from the simplest to the most complex. The background colour refers to CYP1A functional clusters and the substituent that differs from the previous molecule at each step is coloured in magenta.

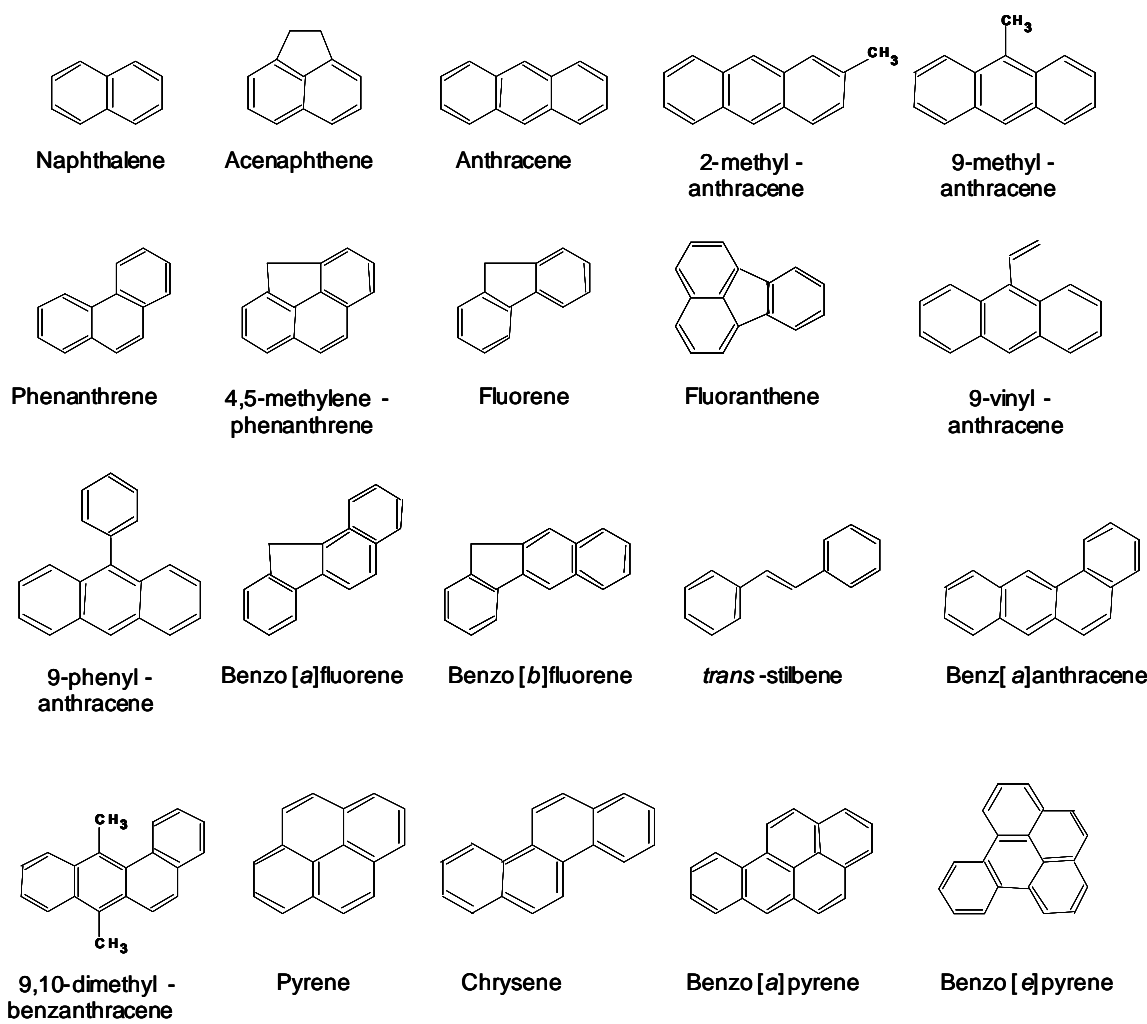
**Fig. (S5).** Structure of the PAH substrates used in this work.

Table S2. Observed rates of metabolite formation measured at a saturating concentration of polycyclic aromatic hydrocarbon substrates. Metabolites were quantified by fluorescence after HPLC separation. Activities were calculated from initial velocities determined from metabolite concentration observed at different incubation times. Enzymes were produced in yeast and incubations were performed with yeast microsomal fractions at which recombinant human microsomal epoxide hydrolase was added. Metabolites were quantified by fluorescence after HPLC separation. Activities units are fluorescence arbitrary units/min/mg of microsomal protein. This table is a non-processed data set

rabbit_1A2	..MAMGPAAPLSVTTELLVSAVFCLVFWAVRAGSRPKVPKG	38
human_1A1	...MLFPFISMATEFILLASVIFCLVFWVIRASRPPVPKG	36
mouse_1A1	MPSMYGLPAPAFVVSATELLLAVATVFCLVGFWMATRTQVPKG	40
human_1A2	..MAISQSVPPFSATELLLLASAIFCCLVFWVL...LRPRPVPKG	38
rabbit_1A2	LKRLPGFWGWPLLGHLLTLGKNFHVAFLSRRYGVVFQI	78
human_1A1	LHNEPGFWGMFLIGHMLTLGKNFHIALSRMSQQYGVVLQI	76
mouse_1A1	LKTPPGFWGLPFIGHMLTVGKNFHLSLTRLSQQYGVVLQI	80
human_1A2	LKSPPPEFWGWPLLGHVLTLGKNFHIALSRMSQRYGVVLQI	78
rabbit_1A2	RIGSTPVVVLSCLDITIMQALVRQGDMIFKGRPDLYSSSFIT	118
human_1A1	RIGSTPVVVLSCLDITIRQALVRQGDDFKGRPDLYSTFLIT	116
mouse_1A1	RIGSTPVVVLSCANTIMQALVRQGDDFKGRPDLYSTFLIT	120
human_1A2	RIGSTPVVVLSCLDITIRQALVRQGDMIFKGRPDLYTSTLIT	118
rabbit_1A2	EGQSMCFSEIISQGPVWAARRRLAQSFIASNPASSSS	158
human_1A1	NGQSMSEFSEIISQGPVWAARRRLAQSFIASDPASSSS	156
mouse_1A1	NGKSMCFMPDSGPVWAARRRLAQNALSFIASDPTASS	160
human_1A2	DGQSMCFSEIISQGPVWAARRRLAQNALSFIASDPASSSS	158
rabbit_1A2	CYLEEHVSKQEAENLISRLQELMAVGRFDPYQSILVVAAR	198
human_1A1	CYLEEHVSKKEAEVLISTLQELMAAGPHFNPYRYVVVSVTN	196
mouse_1A1	CYLEEHVSKKEANLYLVSKLQKVMAEVGVGHFDPYKYLVVSVAN	200
human_1A2	CYLEEHVSKKEAKALISRLQELMAAGPHFDPYQNVVVSVAN	198
rabbit_1A2	VIGAMCFGRHFPQGSEEMLDVVRNSSFVETASSSPVDF	238
human_1A1	VICAICFGRRYDHHNAEILLSIVNHLNNNFGEVVVGSGNPADF	236
mouse_1A1	VICAICFGQRYDHDDQELLISIVNLSNHEFGEVTGSGYPADF	240
human_1A2	VIGAMCFGQHFPESSDEMMLSLVKNNTHEFVETASSGNPLDF	238
rabbit_1A2	FPIILRYLPNRPQLQRFKDNQRFILRFLQKTVREHYEDFDRN	278
human_1A1	IPIILRYLPNPSLNAFFQNLNEKFYSFNQHMKVEEYKTFERG	276
mouse_1A1	IPVILRYLPNSSLDAFFQNLNDKFYSGMOKLIKERYR7FEXG	280
human_1A2	FPIILRYLPNPAIQLQRFAFNQRFILWFLQKTVQEHYQDFDKN	278
rabbit_1A2	SIQDITGALFKHSEKNSKANGGLIQ..EKIVNLVNDIFG	316
human_1A1	HIRDITDSLIEHCQEQKLDENANVQLSDEKIINIVLDLIFG	316
mouse_1A1	HIRDITDSLIEHCQEQKLDENANVQLSDDDKVITIVLDLIFG	320
human_1A2	SVRDITGALFKHSEKKGPRASGNLIPQ..EKIVNLVNDIFG	316
rabbit_1A2	AGFDUTITALLSWSIMYLV...[blue]I[blue]N[blue]Q[blue]R[blue]K[blue]I[blue]C[blue]E[blue]LD[blue]A[blue]V[blue]V[blue]G[blue]R[blue]P[blue]Q[blue]Q	356
human_1A1	AGFDUTITALLSWSIMYLV...I[N]Q[R]K[I]C[E]L[D]A[V]V[G]R[P]Q[Q]	356
mouse_1A1	AGFDUTITALLSWSIMYLV...I[N]Q[R]K[I]C[E]L[D]T[V]I[G]R[D]R[Q]	360
human_1A2	AGFDUTITALLSWSIMYLV...I[N]Q[R]K[I]C[E]L[D]T[V]I[G]R[D]R[Q]	356
<u>J helix</u>		
rabbit_1A2	PRLSDRPQLPYLEAFFILELFRTSH...FTIIPHSTTRDTTL	396
human_1A1	PRLSDRSHLFYMFATFILETFRHSSF...FTIIPHSTTRDTSL	396
mouse_1A1	PRLSDRPQLPYLEAFFILETFRHSSF...FTIIPHSTTRDTSL	400
human_1A2	PRLSDRPQLPYLEAFFILETFRHSSF...FTIIPHSTTRDTTL	396
rabbit_1A2	NGFHIPKECCIFINQWQINHDQPLQNLGDPEEFPERFLTAD	436
human_1A1	KGFYIPKGRCVFNQWQINHDQKLNVNPSEFLPERFLPD	436
mouse_1A1	NGFYIPKGCCVFVNQWQVNHDRELMGDPSEFRPERFLPS	440
human_1A2	NGFYIPKKCCVFVNQWQVNHDPELWEDPSEFRPERFLTAD	436
rabbit_1A2	GAINKPLSEK...[blue]L[blue]F[blue]G[blue]L[blue]G[blue]K[blue]R[blue]C[blue]I[blue]G[blue]E[blue]L[blue]A[blue]R[blue]W[blue]E[blue]L[blue]F[blue]L[blue]A[blue]I[blue]L[blue]L	476
human_1A1	GAIDKV.LSEK...I[blue]F[blue]G[blue]M[blue]G[blue]K[blue]R[blue]C[blue]I[blue]G[blue]E[blue]L[blue]A[blue]R[blue]W[blue]E[blue]L[blue]F[blue]L[blue]A[blue]I[blue]L[blue]L	475
mouse_1A1	GTLDKR.LSEK...[blue]L[blue]F[blue]G[blue]L[blue]G[blue]K[blue]R[blue]C[blue]I[blue]G[blue]E[blue]L[blue]A[blue]R[blue]W[blue]E[blue]L[blue]F[blue]L[blue]A[blue]I[blue]L[blue]L	479
human_1A2	GTAINKPLSEK...[blue]L[blue]F[blue]G[blue]M[blue]G[blue]K[blue]R[blue]C[blue]I[blue]G[blue]E[blue]L[blue]A[blue]R[blue]W[blue]E[blue]L[blue]F[blue]L[blue]A[blue]I[blue]L[blue]L	476
rabbit_1A2	QLEFSVPPGVVVDLTFIYGLTHKHPRCEHVQARPPFSQ	516
human_1A1	QREVFSPVPLGVKVDMTPIYGLTHKHACCEHFQMQLRS...	512
mouse_1A1	QQIEFKVSPGEKVIDMTPTYGLTLKHARCEHFQVQMRSSGP	519
human_1A2	QQLEFSVPPGVVVDLTFIYGLTHKHARCEHVQARPPFSIN.	515

Fig. (S6). Multiple alignment of CYP1A amino acid sequences with positions characterizing differential steroid specificity coloured in blue. The J helix element is underlined.